ADVANCED OPTICAL MATERIALS
www.advopticalmat.de

Fullerene Photodetectors with a Linear Dynamic Range of 90 dB Enabled by a Cross-Linkable Buffer Layer

*Fawen Guo, Zhengguo Xiao, and Jinsong Huang**

Organic photodetectors have attracted significant attention for their immediate application to the replacement of conventional devices based on expensive inorganic semiconductors. Potential new uses in both civil and defense applications take advantage of organic photodetectors' light weight, flexibility, and excellent form factors.[1] An example of a unique application for an organic photodetector is the capability to form organic thin film devices on curved surfaces for things such as an artificial eye and a hemispherical array detector for imaging (HARDI), which allows a very wide field of view without the aberrations encountered in a flat focal plane.[2] In addition to the low cost of materials and the fabrication process, which is the typical advantage of organic electronic devices, organic photodetectors have the potential to outperform their inorganic counterparts; because their low conductivity enables them to dramatically reduce noise. A recent study shows that polymer-based organic photodetectors can have higher sensitivity than traditional photodetectors, such as silicon and InGaAs photodetectors in some wavelength range.[3]

The response characteristics, such as linearity, to very weak light are of ultimate importance when detectivity of organic photodetectors reaches the parity with traditional photodetectors. Recent studies on organic photodetectors have focused on improving detectivity, but little attention was paid to the linearity of the organic photodetector's responsivity, especially in a low light intensity region. The reported detectivities were mostly calculated according to the organic photodetector's reponsivity at relatively strong light levels: orders of magnitude larger than the calculated noise equivalent power (NEP). It has not been shown yet whether the organic photodetectors can still maintain the high responsivity at low incident light intensity close to the NEP. However, there is concern that the organic photodetector would loss its high responsivity at such a low light level as there is generally a much higher density of charge traps in organic rather than inorganic semiconductor materials due to the amorphous or polycrystalline organic semiconductors used. When the charge density generated by the incident light is comparable to the charge trap density, the photogenerated charges might be trapped rather than contribute to the device photocurrent. In this paper, we report on a highly sensitive, fullerene-based organic photodetector device which shows linear response from the indoor light intensity all the way down to 12 pW m^{-2}. This type of organic photodetector presents a linear dynamic range of 90 dB.

Our first step is to fabricate a photodetector with very small noise current so that the weak light generated small photocurrent can be distinguishable from the noise current. The light-absorbing material used in this study is fullerene (C_{60}) which is one of the most broadly studied materials for devices, including organic solar cells and organic field effect transistors, because of its excellent optoelectronic properties, such as a large light absorption coefficient, of 1.21×10^5 cm^{-1} at 442 nm,[4] and high electron mobility, of up to 6~11 cm^2 V^{-1} s^{-1}.[5] In our organic photodetector devices, the thickness of C_{60} is around 80 nm which allows more than 60% of the light above its optical bandgap to be absorbed. In our previous study, it was found that C_{60} is a good photoconductor material with much longer hole trapping time than electron transit time. A photoconductive gain above 50 under reverse bias below –5 V has been observed in the device with a structure of indium tin oxide (ITO)/poly(3,4-ethylenedioxythiophene):poly(styrenesulfonate) (PEDOT:PSS) (35 nm)/C_{60} (80 nm)/2,9-dimethyl-4,7-diphenyl-1,10-phenanthroline (BCP) (20 nm)/aluminium Al (100 nm).[6] The high gain can be explained by the trapped-hole-enhanced electron-injection process: the photogenerated holes tend to be trapped at the interface of PEDOT:PSS and C_{60} layers, because C_{60} is a poor hole transport material. The high density trapped holes induce the band-bending in C_{60} at the interface of PEDOT:PSS and C_{60} layers. They also reduce the electron injection barrier dramatically, which eventually leads to strong secondary electron injection from PEDOT:PSS to C_{60}. One trapped hole can induce the injection of more than one electron which generates the gain and such mechanism was also observed in another type of nanocomposite photodetector in our previous study.[6,7] Despite of the high gain, these organic photodetector devices are not suitable for weak light detection because they suffer from high dark-current up to 2 mA cm^{-2} at –6 V. Although there is a large electron injection barrier of 0.6 eV from PEDOT:PSS to C_{60} under reverse bias, the electron injection was enormously strong under reverse bias. This large dark-current might originate from the leakage current due to the thin, rough C_{60} layer and the broadening of the C_{60}'s lowest unoccupied molecule orbital (LUMO) of amorphous C_{60} film on the surface of PEDOT:PSS. Therefore increasing the thickness of C_{60} film won't be able to reduce the dark-current significantly. This strong electron injection provides the required ohmic contact for the photoconductive gain but, on the other hand, results in large noise current. In addition, both the C_{60} and BCP layers

F. Guo, Z. Xiao, J. Huang
Department of Mechanical and
Materials Engineering and
Nebraska Center for Materials and Nanoscience
University of Nebraska-Lincoln
Lincoln, Nebraska, 68588, USA
E-mail: jhuang2@unl.edu

DOI: 10.1002/adom.201200071

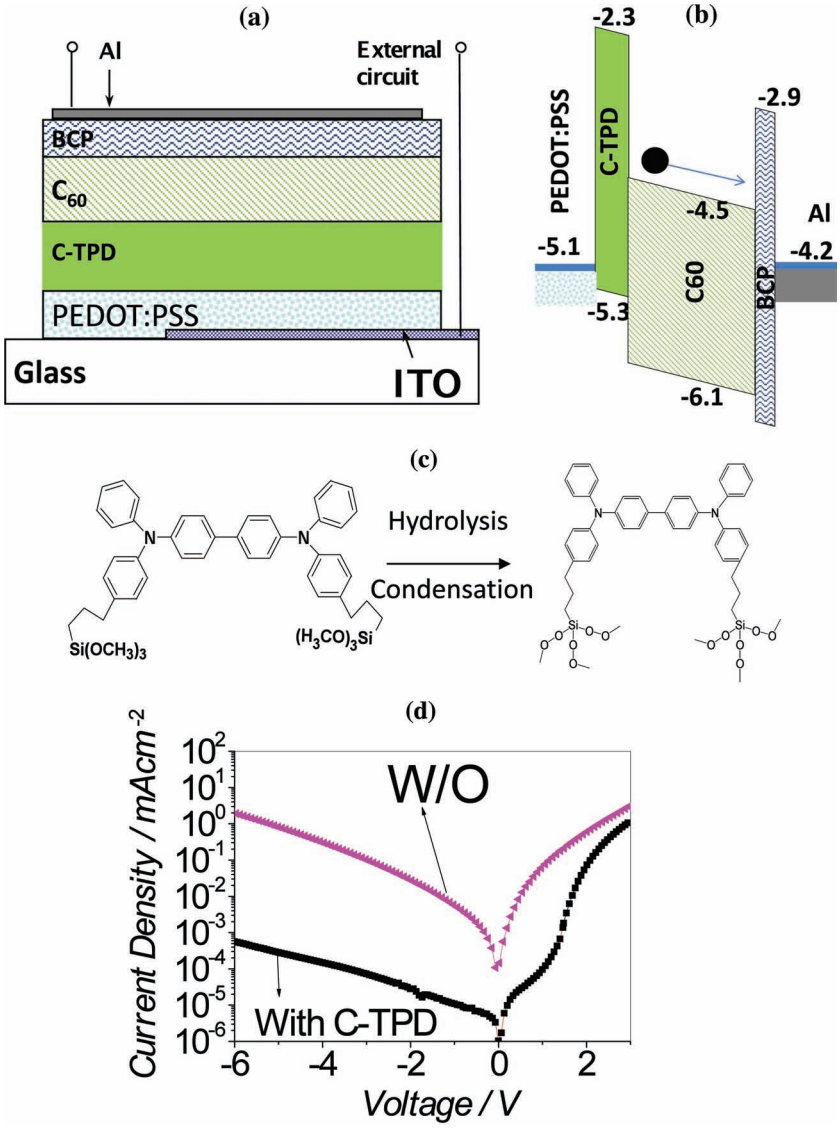

Figure 1. (a) Device structure and (b) the energy diagram of the fullerene based organic photodetector with C-TPD buffer layer; (c) the hydrolysis condensation process of C-TPD in air for the cross-linking of TPD; (d) dark-current of the fullerene based organic photodetector with or without C-TPD buffer layer.

are good electron transport materials, which help to conduct the large electron leakage current. In this work, we successfully reduced the dark-current by 3~4 orders of magnitude, by using a buffer layer of cross-linked 4,4'-Bis[(p-trichlorosilylpropylphenyl)phenylamino]-biphenyl (C-TPD) at the interface of PEDOT:PSS and C_{60}. The device structure of ITO/PEDOT:PSS (35 nm)/C-TPD (25 nm)/C_{60}(80 nm)/BCP (20 nm)/Al (100 nm) is shown in **Figure 1**(a).

C-TPD has been studied in organic light-emitting diodes as an anode modification layer and hole injection/transport layer.[8] C-TPD is a good hole transport material, but it has poor electron mobility. This C-TPD layer introduces a high electron injection barrier of 2.8 eV, which can greatly reduce the dark current, as shown by the energy diagram in Figure 1(b).[9,10] The molecular structure and cross-linking process of the C-TPD layer is shown in Figure 1(c), which is a thermal annealing-assisted hydrolysis process.[11] The insertion of a C-TPD layer was found to reduce the dark-current density by three to four orders of magnitude compared with the control device without a buffer layer, as shown in Figure 1(d).

In addition to increasing the electron injection barrier and suppressing electron transport, the cross-linked TPD at the ITO side is also expected to reduce the leakage current and eliminate catastrophic shorts by forming a condensed, smooth, conformal, and pinhole free buffer layer on top of PEDOT:PSS.[10] In order to verify the role of this buffer layer in reducing the roughness of ITO and C_{60} layer, the surface roughness of each layer was measured with AFM. The stacking layer of ITO/PEDOT:PSS (35 nm)/C-TPD (25 nm)/C_{60}(80 nm) and the AFM images over the area of 1 μm × 1 μm are shown in **Figure 2**. The commercial ITO is rough, with an average roughness of 4.547 nm. The spin-coated PEDOT:PSS layer can reduce the roughness of an ITO surface by almost three times; and the C-TPD layer can further reduce the roughness by four times, resulting in a very smooth surface with a roughness of 0.407 nm. A much smoother surface with a C-TPD buffer layer also improves the film quality of the C_{60} layer. As shown in Figure 2, the C_{60} layer on C-TPD is twice as smooth as the C_{60} layer on PEDOT:PSS. The more smooth and condensed C_{60} film should also contribute to the dramatically reduced small dark-current observed because of the reduced degree of disorder in C_{60}.

The dark-current reduction in our devices should ascribe to the two factors: one is the introduced high electron injection barrier at the PEDOT:PSS/C-TPD interface, and the other is the reduced leakage current and catastrophic shorts due to the inserted compact C-TPD buffer layer and improved film quality of C_{60}. To find out which dominates the dark-current reduction, a series of devices were fabricated with different C-TPD thicknesses. In addition, a series of devices with a non-crosslinking polymer, polyvinylcarbazole (PVK) were also fabricated as the buffer layer. PVK was chosen here because it has comparable LUMO level with that of C-TPD, but does not has as good film forming capability as C-TPD. Therefore such comparison is expected to distinguish the contribution of dark-current reduction from the two factors.

Figure 3 shows the dark-current of the devices at reverse bias of –6 V with different buffer layer thickness using C-TPD and PVK as buffer layers. It can be seen that inserting as thin as 15 nm C-TPD can reduce the dark-current of the C_{60} based photodetector by three orders of magnitude. Increasing the thickness of C-TPD up to 80 nm results in further reducing of the dark-current but by less than one order of magnitude.

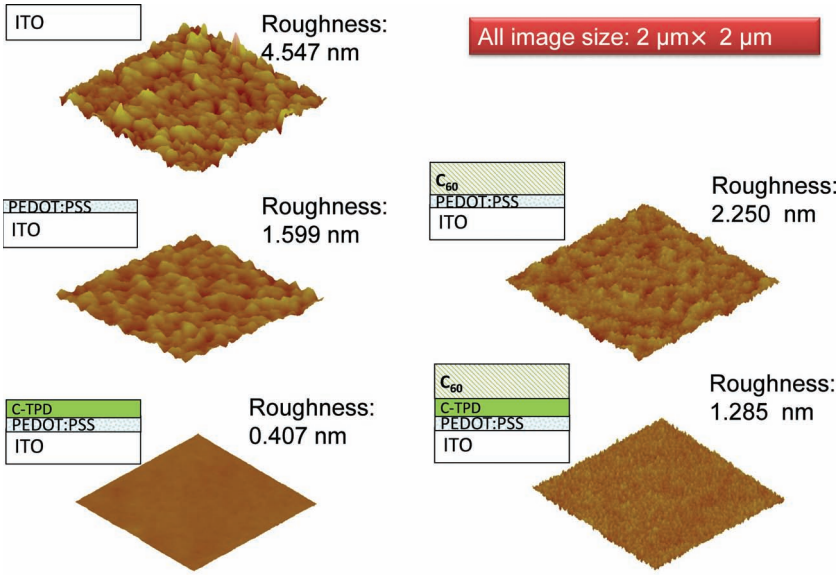

Figure 2. AFM images of the surface with film stacking structure shown in the figure as well. Surface roughness is also labeled for each film surface.

Although a thick C-TPD reduces the device dark-current, it also reduce the external quantun efficiency (EQE) and the device response speed. All the device characteristis shown below are from the device with 25 nm C-TPD which gives a compromised combination of low noise and large external quantum efficiency and fast response speed. The photodector devices using PVK buffer layer would have the same the dark-current with that with C-TPD buffer layer because of the introduced same energy barrier, if the dark-current reduction is solely caused by the introduced energy barrier. However, the dark-current of the devices with PVK buffer layer is two orders of magnitude higher than the device with C-TPD layers with same buffer layer thickness. Increasing the thickness of PVK is not effective to reduce the dark-current since 80 nm thick PVK doesn't give as low dark-current as 15 nm C-TPD. It is expected that the film quality of PVK is not good enough to exclude possible current leakage even when it is as thick as 80 nm. The results shown here indicate that although a large energy barrier can effectively reduce the charge injection and thus dark-current, a prerequisite is the film should be compact enough so that the leakage current won't occur. It is thus concluded both factors contribute to the dark-current reduction in our devices and C-TPD combines these two very well.

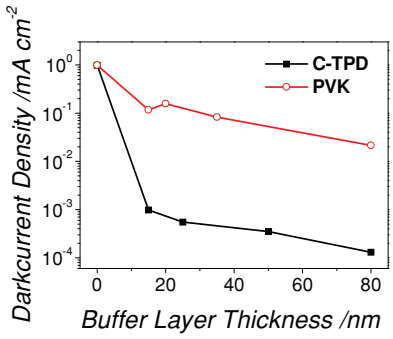

Figure 3. Dark-current density of the C_{60} based photodetetors at the bias of –6 V using buffer layer of C-TPD and PVK of different thickness.

The lowest detectable light by a photodetector is characterized by NEP, which is the lowest light power needed to distinguish the photocurrent from noise current. The NEP of a photodetector can be described as:[12]

$$NEP = \frac{(2e\bar{i}_b + 2e\bar{i}_d + 4k_B T/R)^{1/2}}{R_{es}} B^{1/2} \quad (1)$$

where e is the elementary charge, i_b is the photocurrent generated by background radiation, i_d is the the dark-current, k_b is the Boltzmann constant, T is the tempreture in kelvin, R is the resistance of the detector, R_{es} is responsivity, and B is the bandwidth. For the photodetector working in UV-Vis regions, i_b can be neglected compared to the other two noise sources. Responsivity can be calculated from the measured external quantum efficiency (EQE) by

$$R_{es} = EQE/h\nu \quad (2)$$

where $h\nu$ is the energy of the incident photon in terms of electron-volts. To find out the NEP for this type of organic photodetctors, the noise current was measured with a Stanford Research SR830 Lock-In amplifier following the method reported by G. Konstantatos et al.[13] In order to be consistent with the EQE measurement, the lock-in frequency of the noise current was set to be 35 Hz, the same as the modulation frequency in the EQE measurement. **Figure 4**(a) shows the noise current vs. the dark-current. The shot noise limit and thermal noise limit calculated are also shown in the figure for comparison.[12] The measured noise current was found to be a little higher but very close to the shot noise limit. It is clear that the detector's noise was dominated by dark-current noise (shot noise). Therefore, in order to detect weak light, it is crucial to reduce the dark-current of organic photodetectors.

The measured EQE curves of the fullerene based organic photodetectors with C-TPD buffer layer are shown in Figure 4b at different applied reverse bias. The highest EQE at –6 V is close to 40%. It is clear that the insertion of a C-TPD layer eliminates the photoconductive gain. The inserted C-TPD layer interrupts the ohmic contact at the PEDOT:PSS/C_{60} interface, as evident from the rectifying type dark-current curve shown in Figure 1d. Therefore, there is no continuous supply of electrons for the photoconductive gain. From another prospective, the inserted C-TPD layer eliminates the trapped-hole-enhanced electron injection from PEDOT:PSS to C_{60} because C-TPD is too thick for the tunneling of electrons even though the hole can still be trapped in C_{60}. However, the insertion of this layer does increase the sensitivity of the fullerene based organic photodetector yielding a much smaller NEP and larger specific detectivity due to the dramatically reduced noise current. The NEP is calculated to be 0.55 pW which is ten times smaller than the fullerene based organic photodetector without the buffer layer.

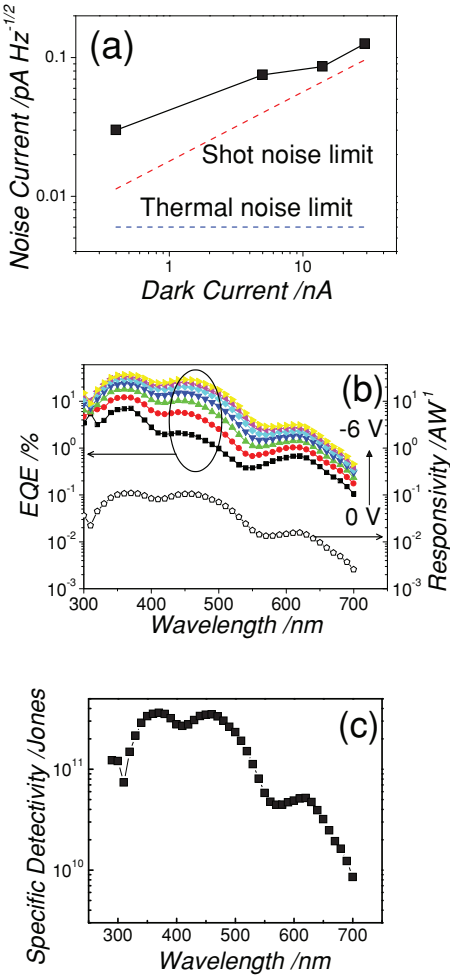

Figure 4. The measured noise current (a) and EQE (b) of the fullerene based organic photodetectors with a C-TPD buffer layer at 35 Hz under different dark-current or bias, respectively. The responsivity of the photodetectors under the bias of –6 V is also shown in (b). (c) The calculated specific detectivity of fullerene based organic photodetectors with a C-TPD buffer layer.

The specific detectivity gives a fair comparison of different photodetectors by normalizing the device area:[3,14]

$$D^* = (AB)^{1/2}\mathrm{R_{es}}/i_n\ (Jones) \quad (3)$$

where A is the effective detector area in cm^2, $B$is the bandwidth, $R_{es}$is responsivity, and i_n is the measured total noise current. D^* is proportional to R_{es} and inversely proportional to the noise current. Although the responsivity of the C_{60} based photodetector was reduced by two orders of magnitude with the inserted C-TPD buffer layer compared to our previous photoconductive type C_{60} based photodetector, the dark-current was decreased by more than three orders of magnitude. Therefore the specific detectivity, or sensitivity of the C_{60} based photodetector, has been increased by 1 order of magnitude in this work. The peak D^* of the photodetector reaches 3.6×10^{11} Jones at 370 nm, as shown in Figure 4(c), which is more than ten times higher than the control device without the C-TPD buffer layer.

The upper limit of the fullerene based organic photodetector response speed is limited by the electron transit time from the anode to the cathode side which is determined by the applied bias (V), thickness of the C_{60} film (d), and the mobility of electrons in C_{60}(μ_e):

$$\tau_t = d^2/\mu_e V \quad (4)$$

The calculated transit time is 1 ns under reverse bias of –6 V using a moderate electron mobility of 0.01 $cm^2\ V^{-1}\ s^{-1}$. The measured response time can be limited by the RC constant of the measurement circuit. The response speed was measured using a chopped light pulse recorded by an oscilloscope, as shown in **Figure 5**(a). The RC time constant of the circuit is calculated to be 10~30 μs. And the shutter switching on (off) time is 50 μs, which is calculated from the spin-rate of the chopper. The device shows a rise and decay time of 50 μs which is clearly limited by the slow shutter switching on (off) speed. The response speed of the fullerene based organic photodetector is quicker than 50 μs (20 kHz).

As decribed above, the specific detectivity of our devices was calculated using the EQE measured at a relatively large incident light intensity of ~μWcm^{-2}. So direct comparison of specific detectivity might not tell the exact capability of a photodetector to detect the weak light with light intensity approaching NEP. In practical applications, a constant responsivity from strong light all the way down to weak light is critically important so that an organic photodetector can be applied for weak light sensing. Every photodetector only has a finite range of linear response and is characterized by linear dynamic range (LDR) in which the responsivity keeps constant. In inorganic photodetectors, LDR is limited by NEP at the weak light end and by saturation of photocurrent at the strong light end. But this senario does not necessarily hold for organic photodetectors because of the existing of large density of charge traps in most non-single crystal organic semiconductors.

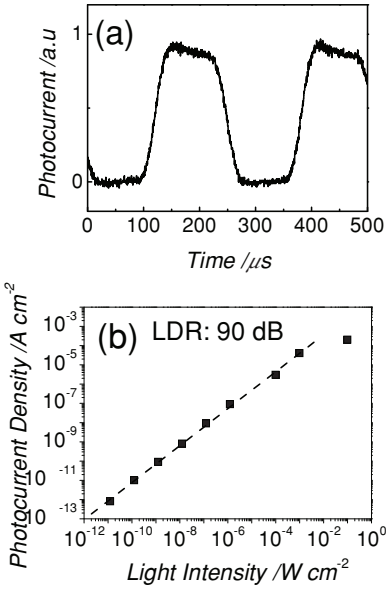

Figure 5. Response speed (a) and linear dynamic range (b) of the fullerene based organic photodetectors with a C-TPD buffer layer. The slope of the fitting line in (b) is 0.96.

Here, the LDR of the fullerene based organic photodetectors was directly measured by recording photocurrent under modulated illuminations from strong light intensity of 0.1 Wcm^{-2} all the way down to NEP. The photocurrents of the fullerene organic photodetector device under different light intensities were recorded with a Lock-In Amplifier SR830 at a frequency of 35 Hz, and the result is shown in Figure 5(b). The lowest detectable light intensity is 12 $pWcm^{-2}$, with an effective device area of 0.05 cm^2, yielding a detectable power of 0.6 pW, which is very close to the calculated NEP of the C_{60} based photodetectors. This is the first time an organic photodetector with a linear response at such a low level light intensity has been reported. The photocurrent saturated at high light intensity reaches 0.1 Wcm^{-2}. The fullerene organic photodetector device with a buffer layer has a linear response to varied light intensity by nine orders of magnitude, corresponding to a LDR of 90 dB. This high LDR is larger than those of many inorganic photodetectors, such as GaN (50 dB)[15] and InGaAs (66 dB)[3] and approaches that of silicon photodetectors (120 dB).[3] It is also among the highest reported LDRs for both small molecule and polymer-based organic photodetectors.[3,16]

It is not clear yet why the fullerene based organic photodetector has such a good linear response at such a low level of light, but it is expected that the following three factors should contributed to this large LDR observed in C_{60} based photodetectors here: 1) excellent electron transport property of fullerene;[5] 2) much more efficient free electron generation from Wannier exciton under small electric field in fullerene than any other organic semiconductor acceptor;[17] 3) the low density electron trap density in fullerene. The light intensity dependent of photocurrent was fitted by a line with a slope of 0.96. The slightly deviation of the slope from 1 indicates there is still charge recombination in the photodetector. Since the photodetector device works under a high reverse bias of –6 V, it is expected that the bimolecular recombination, charge transfer exciton recombination or trap-assisted electron recombination should not dominate the recombination. While monomolecular recombination, such as Frenkel exciton recombination, is likely considering the relative thick C_{60} film of 80 nm and non-purified C_{60} used. It also indicates a path to future increase the performance of current C_{60} based photodetector by exploring the growth of highly crystalline C_{60} for higher speed, lower noise, and larger LDR organic photodetectors.

In summary, the dark-current of the photodetector has been successfully reduced by a C-TPD buffer layer. The high detectivity of 3.6×10^{11} Jones at 370 nm and the wide LDR of 90 dB, along with a response speed faster than 20 kHz, suggests that the fullerene based organic photodetectors reported here can open the way for many potential applications, such as replacing the CCD array in a digital camera. The high sensitivity of this type of photodetector, particularly in the UV range, makes it potentially useful in monitoring the weak UV emission from scintillators which generally give UV emission.

Experimental Section

C_{60} was purchased from Nano-C; BCP was purchased from SIGMA-ALDRICH; PEDOT:PSS was purchased from H.C.STARCK; All materials were used as received without any purification. TPD-Si_2 was synthesized following the route from literature.[18] For the device fabrication, PEDOT:PSS was first spin-coated onto a cleaned ITO glass substrate at a spin speed of 3000 rpm, and then baked at 120 °C for 30 min; TPD-Si_2 was first spin coated on the top of a PEDOT:PSS layer and then thermally annealed at 110 °C for 1 h in air to get it cross-linked; C_{60}, BCP and aluminium were deposited by thermal evaporation. The active device area is 0.05 cm^2 which is defined by the shadow masks.

The shot noise limit is calculated by $i_{n,sh} = \sqrt{2e\,B i_d}$, where e is the elementary charge, B is the modulated bandwidth, i_d is the dark current. The thermal noise limit is calculated by $i_{n,th} = \sqrt{\frac{4k_B\,T\,B}{R}}$, where k_B is Boltzmann constant, T is the absolute temperature, B is the modulated bandwidth, R is the resistance of the detector.

For the device dynamic range measurement, different light sources were used to provide a large variation of light intensity by ten orders of magnitude. For light intensity below 1 μWcm^{-2}, the monochromatic light was provided by a 350 nm LED powered by a function generator. For stronger light intensity up to 0.1 Wcm^{-2}, the light was provided by a Xe lamp; and the UV part of the light is calculated by the integration of UV light intensity from the Xe lamp spectrum. The light intensity was first calibrated with a Si diode at the highest light intensity of each light source, and the lower light intensities were obtained by attenuating the strong light with a set of Newport neutral density filters.

Acknowledgments

This work is supported by a US Defense Threat Reduction Agency Young Investigator Award (DTRA YIP, award number HDTRA1–10-1–0098) and Office of Naval Research (ONR, grant no. N000141210556).

Received: December 26, 2012
Published online: February 27, 2013

[1] a) T. Rauch, M. Böberl, S. F. Tedde, J. Fürst, M. V. Kovalenko, G. Hesser, U. Lemmer, W. Heiss, O. Hayden, *Nature Photon.* **2009**, *3*, 332; b) G. A. O'Brien, A. J. Quinn, D. A. Tanner, G. Redmond, *Adv. Mater.* **2006**, *18*, 2379; c) P. Peumans, V. Bulović, S. Forrest, *Appl. Phys. Lett.* **2000**, *76*, 3855.

[2] a) H. C. Ko, M. P. Stoykovich, J. Song, V. Malyarchuk, W. M. Choi, C.-J. Yu, J. B. Geddes III, J. Xiao, S. Wang, Y. Huang, J. A. Rogers, *Nature* **2008**, *454*, 748; b) X. Xu, M. Davanco, X. Qi, S. R. Forrest, *Org. Electron.* **2008**, *9*, 1122; c) I. Jung, J. Xiao, V. Malyarchuk, C. Lu, M. Li, Z. Liu, J. Yoon, Y. Huang, J. A. Rogers, *Proc. Nat. Acad. Sci. USA* **2011**, *108*, 1788.

[3] X. Gong, M. Tong, Y. Xia, W. Cai, J. S. Moon, Y. Cao, G. Yu, C. L. Shieh, B. Nilsson, A. J. Heeger, *Science* **2009**, *325*, 1665.

[4] J. P. Hare, Further properties of Buckminsterfullerene, http://www.creative-science.org.uk/propc60.html, accessed: February, **2013**.

[5] a) H. Li, B. C. K. Tee, J. J. Cha, Y. Cui, J. W. Chung, S. Y. Lee, Z. Bao, *J. Am. Chem. Soc.* **2012**, *134*, 2760; b) T. B. Singh, N. S. Sariciftci, H. Yang, L. Yang, B. Plochberger, H. Sitter, *Appl. Phys. Lett.* **2007**, *90*, 213512; c) H. Bräuning, R. Trassl, A. Diehl, A. Theiß, E. Salzborn, A. A. Narits, L. P. Presnyakov, *Phys. Rev. Lett.* **2003**, *91*, 168301.

[6] J. Huang, Y. Yang, *Appl. Phys. Lett.* **2007**, *91*, 203505.

[7] F. Guo, B. Yang, Y. Yuan, Z. Xiao, Q. Dong, Y. Bi, J. Huang, *Nat. Nanotechnol.* **2012**, *7*, 798.

[8] Q. Huang, G. A. Evmenenko, P. Dutta, P. Lee, N. R. Armstrong, T. J. Marks, *J. Am. Chem. Soc.* **2005**, *127*, 10227.

[9] W. B. Im, H. K. Hwang, J. G. Lee, K. Han, Y. Kim, *Appl. Phys. Lett.* **2001**, *79*, 1387.

[10] H. Yan, Q. Huang, J. Cui, J. G. C. Veinot, M. M. Kern, T. J. Marks, *Adv. Mater.* **2003**, *15*, 835.
[11] J. Cui, Q. Huang, J. C. G. Veinot, H. Yan, Q. Wang, G. R. Hutchison, A. G. Richter, G. Evmenenko, P. Dutta, T. J. Marks, *Langmuir* **2002**, *18*, 9958.
[12] *Photonic Devices* (Ed.: J.-M. Liu), Cambridge University Press, UK **2005**.
[13] G. Konstantatos, I. Howard, A. Fischer, S. Hoogland, J. Clifford, E. Klem, L. Levina, E. H. Sargent, *Nature* **2006**, *442*, 180.
[14] P. Staveteig, Y. Choi, G. Labeyrie, E. Bigan, M. Razeghi, *Appl. Phys. Lett.* **1994**, *64*, 460.
[15] M. A. Khan, J. Kuznia, D. Olson, J. Van Hove, M. Blasingame, L. Reitz, *Appl. Phys. Lett.* **1992**, *60*, 2917.
[16] a) G. Konstantatos, J. Clifford, L. Levina, E. H. Sargent, *Nature Photon.* **2007**, *1*, 531; b) G. Yu, G. Srdanov, J. Wang, H. Wang, Y. Cao, A. J. Heeger, *Synth. Met.* **2000**, *111*, 133.
[17] T. Liu, A. Troisi, *Adv. Mater.* **2012**, DOI:10.1002/adma.201203486; B. Yang, F. Guo, Y. Yuan, Z. Xiao, Y. Lu, Q. Dong, J. Huang, *Adv. Mater.* **2013**, *25*, 572.
[18] Q. Huang, J. Li, T. J. Marks, G. A. Evmenenko, P. Dutta, *J. Appl. Phys.* **2007**, *101*, 093101.